Conformational Preferences of the Asparagine Residue. Gas-Phase, Aqueous Solution, and Chloroform Solution Calculations on the Model Dipeptide

Carlos Alemán* and Jordi Puiggalí*

Departament d'Enginyería Química, E.T.S. d'Enginyers Industrials de Barcelona, Universitat Politècnica de Catalunya, Diagonal 647, Barcelona E-08028, Spain

Received: October 31, 1996[⊗]

The conformational preferences of the asparagine dipeptide have been determined in the gas phase using ab initio calculations at the HF/6-31G(d) and MP2/6-31G(d) levels. Geometry optimizations lead to 17 different minima, the lowest energy structure being characterized by a $C_{7,eq}$ backbone orientation and a *gauche* conformation for the side chain. Self-consistent reaction-field (SCRF) calculations using a polarized continuum method have been performed in order to evaluate the effects of the solvent on the conformational preferences of the compound under study. Water and chloroform were the solvents chosen for this purpose. Results show that water solvent exerts a larger influence on the conformational properties of the asparagine dipeptide than chloroform solvent. However, in both solvents the lowest energy structure is the same as that in the gas phase. Finally, the side chain conformations of the characterized minima have been analyzed and compared with experimental data. The *gauche* was the most populated conformer in the three investigated environments. This feature is in excellent agreement with the experimental data reported for peptides and proteins.

Introduction

Force-field methodologies, *i.e.* molecular mechanics (MM), molecular dynamics (MD), and Monte Carlo (MC), are of great importance in the study of the structural, dynamical, and equilibrium thermodynamic properties of proteins. These techniques are based on the implicit assumption that the energy of a system can be represented by an addition of classical terms. The reliability of the calculations based on the force-field techniques depends not only on the formalism used to describe the different contributions to the energy but also on the quality of the parameters incorporated within the force field.

One characteristic that has been widely used for the critical evaluation of force fields has been their ability to reproduce the structures and energies of small model molecules, for which there are comparable experimental and theoretical data. For instance, dipeptides of glycine and alanine have been usually considered as test cases for force fields derived for naturally occurring amino acids.[1−3] The same strategy has been used for other noncoded amino acids like those disubstituted at the C^{α} atom[4−7] and those with a retroamide bond.[8] Unfortunately, high-level ab initio calculations of model diamides are only available for a small number of amino acids. More specifically, within the 20 coded amino acids, high-level theoretical data are only available for diamides of glycine, alanine, valine, and serine.[1−3,9−13] Thus, the lack of accurate theoretical data for model diamides of other amino acids precludes a critical evaluation and a definitive calibration of force fields.

On the other hand, we are particularly interested in the conformational properties of the asparagine (Asn) residue. The side chain of the Asn is the methylenamide group, which together with the backbone amide group results in a sequence of atoms with special conformational properties. This is the $C(=O)C^{\alpha}C^{\beta}C(=O)$, in which one methylene unit is situated between two carbonyl groups (see Figure 1). During these past years we have investigated the effect that the end carbonyl groups have on the conformational preferences of the central methylene units. Thus, structural studies of diamides[14−16] (R−$NHCO(CH_2)_nCONH$−R, $n = 2$, 3, and 4) have been performed in the solid state and *in vacuo* using quantum mechanical calculations. The results indicated that in all cases the central methylene units adopt a *gauche* conformation, which departs from the all-*trans* conformation usually found in the solid state for aliphatic segments. More recently, we have extended our work experience on the folding of methylene units to a set of diketone analogues, which also have a central aliphatic segment[17] (R−$CO(CH_2)_nCO$−R, $n = 2$, 3, and 4). A *gauche* conformation was also found for the central methylene units, indicating that the folding of methylene units is due to the carbonyl groups.

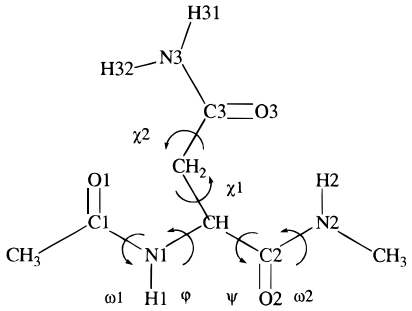

Figure 1. Atomic scheme of AsnD.

A systematic analysis of the side chain conformations of Asn and other related residues like glutamine (Gln) has been recently reported.[18,19] It is based on 24 protein structures determined by X-ray crystallography at a resolution better than 1.5 Å. The results indicated that the *gauche* was the most populated conformation for the methylene units of the side chains, the *gauche/trans* equilibrium being 2.4. However, such study does not clarify if the observed data are due to the intrinsic preferences of the residues or to the chemical environment of the protein, *i.e.* interactions with other residues and/or solvent molecules. The knowledge and understanding of the conformational details in the side chain of coded amino acids could lead to a better understanding of many biological processes. For instance, the conformations adopted by the side chains of Asn and Gln are responsible for the gateing mechanism for ion

[⊗] Abstract published in *Advance ACS Abstracts,* April 1, 1997.

S1089-5647(96)03425-6 CCC: $14.00

passage in channels of phospholipid bilayer membranes[20,21] as well as the interaction with DNA bases in protein−DNA complexes.[22]

In this work, we characterize the minimum energy conformations for a free molecule of the Asn dipeptide (AsnD) using high-level quantum mechanical calculations. Our goals are first to analyze the minimum energy conformations and their relative energy order in the absence of environmental factors. We next investigate the effect of the solvent on the stability of the different minima using a self-consistent reaction-field (SCRF) method. Two different solvents, water and chloroform, were chosen to study the influence of the environment on the molecular system. Finally, we analyze the results on the basis of our previous findings about the folding of methylene units in aliphatic segments located between two carbonyl groups. The results reported in the present work would be useful to test the quality of the parameters incorporated within the force-fields for the Asn residue.

Methods

Gas-Phase Calculations. The AsnD is schematicaly shown in Figure 1. An exploration of the conformational space was performed in order to characterize the minimum energy structures of this compound. Since each of the three flexible dihedral angles φ, ψ, and χ_1 (see Figure 1) are expected to have three minima, 27 minima may be anticipated for the potential energy surface $E = E(\varphi,\psi,\chi_1)$. All these structures were taken as starting points in HF/3-21G[23] geometry optimizations. The χ_2 dihedral angle was initially considered in the all-*trans* conformation, as it is usually observed in peptides and proteins.[18,19] Previous studies suggested that the HF/3-21G level is appropriate for performing the scanning of the potential energy surface, but reoptimization at higher levels of theory and single-point calculations considering electronic correlation effects are required.[10,24,25] Therefore, all the minima characterized at the HF/3-21G level were subsequently reoptimized at the HF/6-31G(d)[26] level. Møller−Plesset perturbation treatment[27] at the MP2/6-31G(d) level was used to compute electron correlation energy. Frequency analyses were performed to verify the nature of the minimum state of the stationary points located during geometry optimizations, as well as to obtain zero-point energies (ZPE) and thermal corrections to the energy.

Solvent-Phase Calculations. The free energies of solvation (ΔG_{sol}) were determined using a semiempirical AM1 adapted version[28−30] of the SCRF developed by Miertus, Scrocco, and Tomasi[31,32] (MST/AM1). According to this method, the ΔG_{sol} was determined as the addition of electrostatic and steric contributions (eq 1). The steric component was computed as the sum of the cavitation and van der Waals terms.

$$\Delta G_{sol} = \Delta G_{ele} + \Delta G_{cav} + \Delta G_{vdW} \quad (1)$$

The cavitation term was determined using Pierotti's scaled particle theory,[33] while the van der Waals term (eq 2) was evaluated by means of a linear relation with the molecular surface area:[28−30]

$$\Delta G_{vdW} = \sum_i \xi_i S_i \quad (2)$$

where S_i is the portion of the molecular surface area belonging to atom i and ξ_i is the hardness of atom i. Parameters defining the hardness of the different atom types in water and chloroform solvents were determined in previous parametrizations.[28c,34]

The electrostatic interaction between the solute and the solvent was computed using the MST-SCRF approach, in which the solvent is represented as a continuous dielectric, which reacts against the solute charge distribution, generating a reaction field (V_R). The effect of the solvent reaction field on the solute is introduced as a perturbation operator in the solute Hamiltonian (eq 3).

$$(H^0 + V_R)\psi = E\psi \quad (3)$$

The perturbation operator is computed in terms of a set of point charges located at the solute/solvent interface, *i.e.* the solute cavity (eq 4).

$$V_R = \sum_i q_i/|r_0 - r| \quad (4)$$

Such imaginary charges were determined by solving the Laplace equation at the solute/solvent interface. In all cases the solute/solvent interface was determined using a molecular shape algorithm.[28−30,34] Standard van der Waals radii (C = 1.5 Å; N = 1.5 Å; O = 1.4 Å; H = 1.2 Å; H(bound to polar atoms) = 0.8 Å) were used.[28b,c]. Since the change of the molecular geometry upon solvation has a negligible effect on the thermodynamic parameters, only gas-phase optimized geometries were used.[15,35] Previous studies indicated that the root mean square deviations between the experimental values of ΔG_{sol} and the values estimated at the MST/AM1 level are 1.0 and 0.40 kcal/mol for water[29] and chloroform[34] solvents, respectively.

Gas-phase calculations were performed with the Gaussian-94[36] computer program. MST/AM1 calculations were performed with an adapted version of MOPAC93 Revision 2,[37] which permits MST calculations with water and chloroform solvents. All the calculations were run on a IBM-SP2 at the Centre de Supercomputació de Catalunya (CESCA).

Results and Discussion

Gas-Phase Calculations. Geometry optimizations at the HF/3-21G level resulted in 19 minima, which were reoptimized at the HF/6-31G(d) level, providing 17 different minima. Thus, two of the minima found at the HF/3-21G level dissapeared upon geometry optimization at the HF/6-31G(d) level, indicating that such structures are not real minima. In all cases minima were characterized as such from frequency analyses. Table 1 displays the dihedral angles for all the minima found at the HF/6-31G(d) level, as well as the backbone and side chain conformations associated with such dihedral angles. The backbone conformations were assigned on the basis of previous ab initio calculations:[1−10] $C_{7,eq}$ (seven-membered intramolecular hydrogen-bonded ring; $\varphi,\psi \approx -60°,60°$), $C_{7,ax}$ ($\varphi,\psi \approx 60°,-60°$), C_5 (five-membered intramolecular hydrogen-bonded ring; $\varphi,\psi \approx 180°,180°$), α_L ($\varphi,\psi \approx 60°,60°$), α_R ($\varphi,\psi \approx -60°,-60°$), β ($\varphi,\psi \approx -150°,60°$), α' ($\varphi,\psi \approx -150°,-60°$), and P_{II} ($\varphi,\psi \approx 60°,180°$). On the other hand, the side chain conformation was defined according to the χ_1 dihedral angle and using the common *gauche*$^+$ (g^+), *skew*$^+$ (s^+), *trans* (t), *skew*$^-$ (s^-), and *gauche*$^-$ (g^-) descriptions. Note that eight of the 17 minima are stabilized by intramolecular hydrogen bonds between the two backbone amide groups defining C_7 and C_5 structures. On the other hand, the g^- conformation is the most frequent rotamer in the side chain. Thus, the χ_1 dihedral angle adopts a g^- conformation in seven minima, whereas the g^+ and t rotamers only appear in five and three minima, respectively. Finally, the s^- is the less frequent conformation, being detected in only two minima.

Relative energies in the gas-phase computed for the 17 minima at the HF/6-31G(d) and MP2/6-31G(d) levels are listed in Table 2. Results reveal some important features. First, the

TABLE 1: Dihedral Angles (in deg) and Backbone and Side Chain Conformations[a] (See Text) for the Minimum Energy Structures Characterized at the HF/6-31G(d) Level of AsnD

no.	ω_1	φ	ψ	χ_1	χ_2	ω_2	backbone	side chain
I	−174.1	−85.5	62.6	56.4	120.4	−179.5	$C_{7,eq}$	g^+
II	173.0	−166.4	−177.3	−137.6	93.0	179.9	C_5	s^-
III	−167.3	−129.6	33.6	66.1	143.7	179.6	β	g^+
IV	−174.4	−86.3	74.8	−167.6	−102.7	−176.0	$C_{7,eq}$	t
V	−166.2	−88.8	70.5	−54.9	−108.5	−175.8	$C_{7,eq}$	g^-
VI	165.7	−178.2	−136.5	54.7	−101.6	−179.1	C_5	g^+
VII	163.9	65.3	33.7	−62.0	178.9	−176.3	α_L	g^-
VIII	163.6	−80.0	−16.7	−59.6	111.0	175.7	α_R	g^-
IX	164.5	75.8	−35.2	−62.2	173.9	−176.0	$C_{7,ax}$	g^-
X	−171.2	−166.0	−58.8	34.5	−112.9	−175.5	α'	g^+
XI	−157.2	67.6	−179.1	−147.0	165.2	−174.8	P_{II}	s^-
XII	158.9	53.1	52.3	47.5	93.0	−173.6	α_L	g^+
XIII	167.3	64.9	36.9	−157.0	−129.0	−177.0	α_L	t
XIV	−170.9	−149.6	140.0	−52.4	−88.0	−179.2	C_5	g^-
XV	−156.4	71.1	177.9	−54.0	112.1	−175.4	P_{II}	g^-
XVI	174.4	75.6	−72.1	−165.2	−101.8	173.2	$C_{7,ax}$	t
XVII	168.8	−122.5	−64.6	−63.6	−26.6	−176.4	α'	g^-

[a] Side chain conformations were defined according to the χ_1 dihedral angle.

TABLE 2: Relative Energies (in kcal/mol) for the Minimum Energy Structures[a] of AsnD

no.	HF/6-31G(d)	HF/6-31G(d)[b]	MP2/6-31G(d)	MP2/6-31G(d)[b]
I	0.0	0.0	0.0	0.0
II	0.8	0.8	0.5	0.4
III	2.5	2.1	4.0	3.6
IV	4.4	4.2	5.1	4.9
V	4.6	4.2	5.4	5.0
VI	5.2	5.2	4.2	4.2
VII	5.5	4.8	7.3	6.6
VIII	6.0	5.6	7.4	7.0
IX	6.5	6.0	7.8	7.3
X	6.8	6.6	6.3	6.1
XI	6.9	6.4	8.3	7.8
XII	7.2	6.9	6.4	6.1
XIII	7.3	6.9	8.9	8.4
XIV	8.5	7.9	10.2	9.6
XV	8.8	8.6	10.2	9.9
XVI	10.0	9.8	10.2	9.9
XVII	12.2	11.7	13.0	12.5

[a] Molecular geometries optimized at the HF/6-31G(d) level. [b] Includes corrections for zero-point energy and for translational, rotational, and vibrational energies at the HF/6-31G(d)//HF/6-31G(d) level.

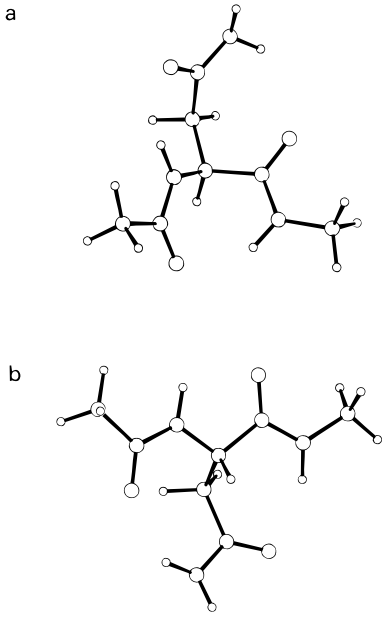

Figure 2. Lowest energy minimum **I** (a) and energy minimum **II** (b) of AsnD.

TABLE 3: Hydrogen-Bonding Geometries for the Interactions between Backbone Amide Groups in the Minimum Energy Conformations of AsnD

no.	type	d(H···O) (Å)	∠N−H···O (deg)
I	C_7	2.096	144.9
II	C_5	2.134	107.6
IV	C_7	2.172	139.5
V	C_7	2.073	144.6
VI	C_5	2.203	107.6
IX	C_7	2.000	148.3
XIV	C_5	2.438	96.7
XVI	C_7	2.049	145.8

lowest energy structure corresponds to the same conformation at the two computational levels. This is a $C_{7,eq}$ structure, in which χ_1 adopts a g^+ conformation (Figure 2a). The next minimum corresponds to a C_5 structure with the side chain in the s^- conformation (Figure 2b). It is destabilized with respect to the lowest energy minimum by 0.8 and 0.4 kcal/mol at the HF/6-31G(d) and MP2/6-31G(d) levels, respectively. We find that the energy difference between the $C_{7,eq}$ and the C_5 is similar to that obtained by other authors for alanine dipeptide. Thus, Gould and Kollman[2] also characterized the $C_{7,eq}$ structure as the lowest energy minimum, the C_5 being 0.4 kcal/mol less stable at the HF/6-31G(d,p)//HF/6-31G(d,p) level. Geometric parameters for the hydrogen bonds between the backbone amide groups of all the C_5 and C_7 conformations are listed in Table 3. As should be expected, the hydrogen-bonding geometric parameters predicted for the C_5 conformations of the AsnD are much more constrained than those predicted for the C_7 conformation.

On the other hand, the agreement between HF/6-31G(d) and MP2/6-31G(d) relative energies is good. Thus, inspection of Table 2 reveals that electron correlation affects only the relative ordering of three conformers: **VI**, **X**, and **XII**. We note that, while in some dipeptides[2,3,38] the electronic correlation effects play a crucial role, in other dipeptides such effects introduce only a small change in the magnitude of the separation between the conformers, but without any change in the ordering.[14,39] Therefore, it is difficult to establish which is the minimum level of theory required to give a good representation of the potential energy surface on small model dipeptides.

Finally, a stricking feature of the potential energy hypersurface $E = E(\varphi,\psi,\chi_1)$ of AsnD is the existence of a large number of intramolecular hydrogen bonds between the amide groups of the side chain and the backbone. Indeed, only four structures (**IX**, **XIII**, **XIV**, and **XVI**), which are destabilized by at least

TABLE 4: Hydrogen-Bonding Geometries for the Interactions between Side Chain and Backbone Amide Groups in the Minimum Energy Conformations of AsnD

no.	atoms	d(H···O) (Å)	∠N−H···O (deg)
I	N1−H1···O3	2.076	132.4
II	N2−H2···O3	2.135	156.2
	N3−H31···O1	2.359	142.4
III	N2−H2···O3	2.495	113.0
IV	N3−H31···O2	2.297	128.6
V	N1−H1···O3	2.222	122.4
VI	N2−N2···O3	2.069	146.8
	N3−H31···O1	2.289	136.9
VII	N1−H1···O3	2.447	107.6
VIII	N1−H1···O3	2.167	129.2
X	N2−H2···O3	2.010	154.6
XI	N2−H2···O3	2.042	148.4
XII	N3−H31···O2	2.248	137.0
XV	N3−H31···O2	2.365	133.2
XVII	N3−H31···O1	2.099	153.5

TABLE 5: MST/AM1 Free Energies of Solvation in Water (ΔG_{sol}) for the 17 Minima of AsnD. Relative Values ($\Delta\Delta G_{sol}$) Are Also Displayed. The SCRF Free Energy Is Decomposed into Electrostatic (ΔG_{ele}) and Steric (ΔG_{ster}) Terms. Conformational Energies Were Estimated by Adding the $\Delta\Delta G_{sol}$ to the Gas-Phase Relativate Energies Computed at the MP2/6-31G(d) Level

no.	ΔG_{ster}	ΔG_{ele}	ΔG_{sol}	$\Delta\Delta G_{sol}$	$\Delta\Delta G_{conf}$
I	4.7	−15.6	−10.9	6.1	0.0
II	4.8	−15.7	−10.9	6.1	0.4
III	4.7	−19.0	−14.3	2.7	0.2
IV	4.7	−18.9	−14.2	2.8	1.6
V	4.7	−18.6	−13.9	3.1	2.0
VI	4.7	−16.4	−11.7	5.3	3.4
VII	4.6	−20.3	−15.7	1.3	1.8
VIII	4.7	−20.3	−15.6	1.4	2.3
IX	4.6	−20.0	−15.4	1.6	2.8
X	4.6	−18.2	−13.6	3.4	3.4
XI	4.5	−19.8	−15.3	1.7	3.4
XII	4.4	−18.4	−14.0	3.0	3.0
XIII	4.5	−21.3	−16.8	0.2	2.5
XIV	4.5	−21.5	−17.0	0.0	3.5
XV	4.7	−18.9	−14.2	2.8	1.6
XVI	4.8	−20.5	−15.7	1.3	5.1
XVII	4.8	−21.2	−16.3	0.7	7.1

7.3 kcal/mol with respect to the lowest energy minimum, do not present such interactions. Hydrogen-bonding parameters for the 13 minima with side chain···backbone interactions are displayed in Table 4. Note that minima **II** (Figure 2b) and **VI**, which adopt a C_5 conformation, present two hydrogen bonds between the side and backbone amide groups, resulting in structures with three intramolecular hydrogen bonds.

Effect of the Aqueous Solvent. The $\Delta\Delta G_{sol}$ values computed in aqueous solution at the MST/AM1 level for the 17 minima characterized at the HF/6-31G(d) level are displayed in Table 5, where the electrostatic and and steric [cavitation + van der Waals] terms are also shown. Results indicate that the electrostatic term provides the most important contribution to ΔG_{sol}, whereas the steric one is unfavorable and adopts a nearly constant value (4.4-4.8 kcal/mol) for all the structures. The largest value of $\Delta\Delta G_{sol}$ is 6.1 kcal/mol, reflecting the strong influence of the aqueous solvent on the potential energy hypersurface $E = E(\varphi,\psi,\chi_1)$ of AsnD. Note that the largest value of $\Delta\Delta G_{sol}$ corresponds to minima **I** and **II**, which have small molecular dipole moments in the gas phase (0.34 and 1.49 D for **I** and **II**, respectively). On the contrary, the lower values of $\Delta\Delta G_{sol}$ correspond to minima **XIII** and **XIV**, which have large molecular dipole moments (4.99 and 4.73 D for **XIII** and **XIV**, respectively). Thus, the alignment of the amide bond dipoles is unfavored in the gas phase due to repulsive interactions between pairs of atoms with charges of equal sign. However, the large molecular dipole moment obtained from the alignment of the bond dipoles provides a more favorable electrostatic interaction with the solvent.

TABLE 6: MST/AM1 Free Energies of Solvation in Chloroform (ΔG_{sol}) for the 17 Minima of the AsnD. Relative Values ($\Delta\Delta G_{sol}$) Are Also Displayed. The SCRF Free Energy Is Decomposed into Electrostatic (ΔG_{ele}) and Steric (ΔG_{ster}) Terms. Conformational Energies Were Estimated by Adding the $\Delta\Delta G_{sol}$ to the Gas-Phase Relativate Energies Computed at the MP2/6-31G(d) Level

no.	ΔG_{ster}	ΔG_{ele}	ΔG_{sol}	$\Delta\Delta G_{sol}$	$\Delta\Delta G_{conf}$
I	−9.0	−3.0	−12.0	1.9	0.0
II	−9.0	−3.0	−12.0	1.9	0.4
III	−9.3	−3.9	−13.2	0.7	2.4
IV	−9.3	−4.1	−13.4	0.5	3.5
V	−9.3	−4.0	−13.3	0.6	3.7
VI	−8.8	−3.2	−12.0	1.9	4.2
VII	−9.2	−4.3	−13.5	0.4	5.1
VIII	−9.4	−4.5	−13.9	0.0	5.1
IX	−9.1	−4.2	−13.4	0.5	5.9
X	−8.7	−3.7	−12.4	1.5	5.7
XI	−9.2	−4.2	−13.4	0.5	6.4
XII	−8.6	−3.7	−12.3	1.6	6.8
XIII	−9.2	−4.7	−13.9	0.0	6.5
XIV	−9.1	−4.5	−13.6	0.3	8.0
XV	−9.0	−4.4	−13.4	0.5	8.6
XVI	−9.0	−4.6	−13.6	0.3	8.3
XVII	−9.1	−4.8	−13.9	0.0	10.6

An estimation of the decisive role of the aqueous solvent on the conformational preferences of AsnD was obtained by computing the conformational free energy ($\Delta\Delta G_{conf}$) in aqueous solution. This was estimated by adding the solution energy $\Delta\Delta G_{sol}$ to the MP2/6-31G(d) gas-phase energy for each conformation. Results are included in Table 5. Although water introduces important changes in the relative energy ordering, the main effect of the solvent is to decrease the energy differences between the conformers. In the gas phase the relative energy ranges from 0.0 to 12.5 kcal/mol, whereas in aqueous solution the conformational free energy ranges from 0.0 to 7.1 kcal/mol. Thus, the potential energy hypersurface $E = E(\varphi,\psi,\chi_1)$ is flatter in aqueous solution than in the gas phase. Note that the lowest energy conformation in aqueous solution is **I**, as in the gas phase. The large unfavorable value of $\Delta\Delta G_{sol}$ estimated for this structure is not enough for its destabilization.

Effect of Chloroform Solvent. Results computed at the MST/AM1 level for the AsnD considering a chloroform solution are shown in Table 6. Comparison with results obtained in aqueous solution reveals important differences. Thus, the steric term is attractive in chloroform solution, whereas in aqueous solution it provides a repulsive contribution. Furthermore, the electrostatic term is the leading contribution in aqueous solution, whereas in chloroform solution it accounts for only 30% of ΔG_{sol}. A similar behavior has been recently found in other organic solvents like carbon tetrachloride.[38,41] Differences displayed by the electrostatic and steric contributions in aqueous and organic solvents must be attributed to the fact that the latter are less structurated than the former.[34,41] However, note that the steric term ranges from −8.6 to −9.4 kcal/mol, whereas the electrostatic contribution ranges from −3.0 to −4.8. kcal/mol. The large range of variation of the electrostatic term indicates that it is decisive for the stabilization of the conformers.

The largest value of $\Delta\Delta G_{sol}$ is 1.9 kcal/mol, indicating that chloroform has a lower influence on the conformational preferences of AsnD than water. The highest value of $\Delta\Delta G_{sol}$ corresponds to minima **I**, **II**, and **VI**, as in aqueous solution calculations. Thus, conformers with large dipole moments are more stabilized by electrostatic interactions with the solvent than those with a small dipole moment.

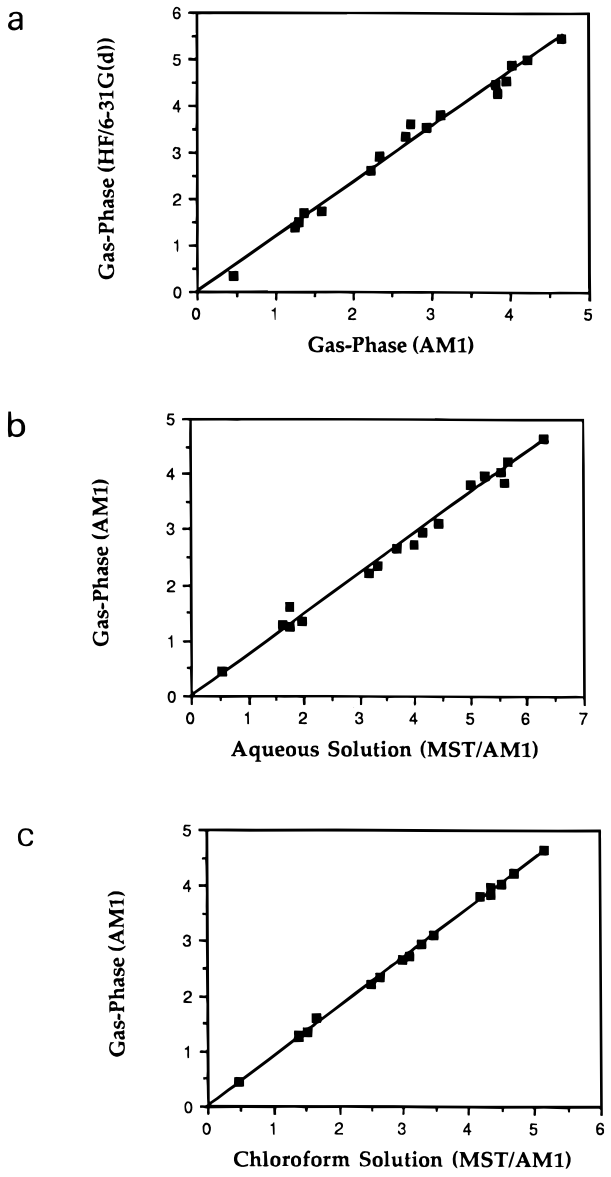

Figure 3. Computed molecular dipole moments: (a) in the gas phase obtained from HF/6-31G(d) and AM1 methods ($\mu_{AM1} = 0.84\mu_{6-31G(d)}$; $r = 0.99$); (b) in the gas phase and aqueous solution obtained from AM1 and MST/AM1 methods, respectively ($\mu_{MST/AM1} = 1.37\ \mu_{AM1}$; $r = 0.99$); (c) in the gas-phase and chloroform solution obtained from AM1 and MST/AM1 calculations, respectively ($\mu_{MST/AM1} = 1.11\mu_{AM1}$; $r = 0.99$).

The conformational free energies in chloroform solution were computed by adding $\Delta\Delta G_{sol}$ to the best estimation of the gas-phase energy. Results are included in Table 6. Note that the conformational free energy ranges from 0.0 to 10.6 kcal/mol. Furthermore, the relative energy ordering is very similar to that obtained in the gas phase. These results point out that although chloroform influences the potential energy hypersurface $E = E(\varphi,\psi,\chi_1)$ of AsnD, the changes are much less dramatic than those induced by water.

Effects of the Solvent on the Dipole Moments. The magnitude of the polarization effects provided by water and chloroform solvents has been estimated by determining the solvent-induced dipole factor. Figure 3 displays the MST/AM1 (solution-phase) *versus* AM1 (gas-phase) dipole moments for the different conformers in aqueous and chloroform solutions, along with the results of a linear regression analysis($y = cx$). Furthermore, gas-phase dipole moments computed at the HF/6-31G(d) and AM1 levels have been also compared in order to support the validity of the latter method.

TABLE 7: Computed[a] and Experimental[b] Populations (in %) of the Different Conformations for the χ_1 Side Chain Dihedral of AsnD

	trans	*gauche*	*skew*
gas phase[c]	12.9	69.2	17.9
aqueous solution	16.6	69.9	13.5
chloroform solution	14.8	68.6	16.6
experimental (proteins)	27.6	66.3	6.1
experimental (peptides)	36.4	63.6	0.0

[a] Estimated using a Boltzmann distribution. [b] From a survey of Asn residues. Reference 19. [c] Gas-phase relative energies computed at the MP2/6-31G(d) level were used (see Table 2).

An excellent correlation ($r = 0.99$) with scaling factor $c = 0.84$ was obtained from the comparison of the gas-phase dipole moments (Figure 3a). This is an expected result since it is known that the AM1 method reproduces reasonably the experimental gas-phase dipole moments,[41] whereas the HF/6-31G(d) method gives an overestimation of such values by 10−20%.[42] The slopes of the plots represented in Figure 3b,c give a quantitative measure of the solvent polarization effect on molecular dipole moments. Results provide an increase of 37% and 11% in water and chloroform, respectively, over gas-phase data. The large change predicted in water by the MST/AM1 method is similar to that obtained by other approaches.[43] Note that the changes induced by chloroform are smaller than those induced by water, although they are nonnegligible. The different behavior found between water and organic solvents was nicely explained by Orozco and Luque in terms of both electrostatic interactions with the solvent and the cavity sizes.[34,40]

Folding of the Methylene Unit in the Side Chain of the Asn Residue. To give an estimation of the conformational equilibrium, the populations of the different conformers found for the χ_1 dihedral angle (Figure 1) of AsnD were computed. For this purpose, the molar ratio of a conformer to the most stable conformer was calculated on the basis of the following relationship: $\exp(-\Delta E/RT)$. Three different populations were estimated: gas phase, aqueous solution, and chloroform solution. A temperature of 298 K was considered in the three cases.

Results obtained for the three environments considered in this work (Table 7) are very similar. The *gauche* is the most populated conformer in all cases (∼70%), the *gauche/trans* equilibrium being 5.4, 4.2, and 4.1 in the gas phase, aqueous solution, and chloroform solution, respectively. These results are in agreement with those previously predicted for diamides[14−16] and diketones,[17] according to which the *gauche* conformation is favored for the bond defined by the first and second carbon atoms next to each of the two carbonyl groups, *i.e.* the C^{α} and C^{β} in the Asn residue. The conformational preferences of the Asn residue in peptides and proteins have been recently characterized from the analysis of crystallographic solved structures.[19] Results obtained from this study have been included in Table 7. Experimental data give support to the theoretical estimations, indicating that the methylene unit of the Asn residue has a clear preference for the *gauche* conformation in proteins. Thus, the frequency for such a conformation was 66% and 64% for proteins and peptides respectively, in agreement with the calculated 69% for the dipeptide model.

Conclusions

We have presented a computational study of the conformational preferences of AsnD in the gas phase, aqueous solution, and chloroform solution. A total of 17 minimum energy conformations were characterized at the HF/6-31G(d) level.

Their gas-phase relative energies have been estimated at the MP2/6-31G(d), ranging from 0.0 to 12.5 kcal/mol. The lowest energy structure corresponds to a $C_{7,eq}$ backbone orientation with a g^+ conformation in the side chain. The effects of the solvents were estimated at the MST/AM1 level. The lowest energy conformation for both aqueous and chloforom solutions was the same as that in the gas phase. However, the two solvents display a very different behavior. Thus, the potential energy hypersurface obtained in chloroform solution is similar to that obtained in the gas phase, whereas that obtained in aqueous solution is flatter. In this case the relative conformational free energies range from 0.0 to 7.1 kcal/mol. This feature must be attributed to the strong stabilization of some conformers in aqueous solution, particularly those with backbone dihedral angles in the helical region of the Ramachandran map. Such conformers present large dipole moments, providing a better electrostatic interaction with the solvent than those stabilized by intramolecular hydrogen bonds between the backbone amide groups.

A detailed analysis of the results indicates that the *gauche* was the most populated conformation for the χ_1 dihedral angle of the Asn residue. This feature is consistent with our previous findings about the folding of methylene units in aliphatic segments located between two carbonyl groups. The present results could help to develop a suitable set of force-field parameters for the side chain of the Asn residue, but taking into account the intrinsic conformational tendencies of the $C(=O)C^{\alpha}C^{\beta}C(=O)$ sequence.

Acknowledgment. The authors express their gratitude to Drs. F. J. Luque and M. Orozco for making available to us their version of MOPAC93 adapted to perform MST calculations. The authors are indebted to the Centre de Supercomputació de Catalunya (CESCA) for computational facilities. The research was supported by DGICYT Project No. PB93-1067 to (J.P).

References and Notes

(1) Böhm, H.-J.; Brode, S. *J. Am. Chem. Soc.* **1991**, *113*, 7129.
(2) Gould, I. R.; Kollman, P. A. *J. Phys. Chem.* **1992**, *96*, 9255.
(3) Gould, I. R.; Cornell, W. D.; Hillier, I. H. *J. Am. Chem. Soc.* **1994**, *116*, 9250.
(4) Barone, V.; Fraternali, F.; Cristinziano, P. L. *Macromolecules* **1990**, *23*, 2038.
(5) Amodeo, P.; Barone, V. *J. Am. Chem. Soc.* **1992**, *114*, 9085.
(6) Alemán, C.; Casanovas, J. *J. Chem. Soc., Perkin Trans. 2* **1994**, 563.
(7) Alemán, C.; Pérez, J. J. *Int. J. Quantum Chem.* **1993**, *47*, 231.
(8) Alemán, C.; Puiggalí, J. *J. Org. Chem.* **1995**, *60*, 910.
(9) Head-Gordon, T.; Head-Gordon, M.; Frisch, M. J.; Brooks, C. L., III; Pople, J. A. *J. Am. Chem. Soc.* **1991**, *113*, 5989.
(10) Shang, N. S.; Head-Gordon, T. *J. Am. Chem. Soc.* **1994**, *116*, 1528.
(11) McAllister, M. A.; Perczel, A.; Csaszar, P.; Viviani, W.; Rivail, J.-L.; Csizmadia, I. G. *J. Mol. Struct. (THEOCHEM)* **1993**, *288*, 161.
(12) Vladia, W.; Rivail, J.-L.; Perczel, A.; Csizmadia, I. G. *J. Am. Chem. Soc.* **1993**, *115*, 8321.
(13) Perczel, A.; Farkas, O.; Csizmadia, I. G. *J. Comput. Chem.* **1996**, *17*, 821.
(14) Navarro, E.; Alemán, C.; Puiggalí, J. *J. Am. Chem. Soc.* **1995**, *117*, 7307.
(15) Alemán, C.; Navarro, E.; Puiggalí, J. *J. Org. Chem.* **1995**, *60*, 6135.
(16) Navarro, E.; Alemán, C.; Puiggalí, J. *Biopolymers* **1995**, *36*, 711.
(17) Alemán, C.; Navarro, E.; Puiggalí, J. *J. Phys. Chem.*, in press.
(18) Alemán, C.; Vega, M. C.; Navarro, E.; Puiggalí, J. *J. Pept. Sci.*, in press.
(19) Vega, M. C.; Alemán, C.; Navarro, E.; Puiggalí, J. Submitted work.
(20) Karle, I.; Flippen-Anderson, J. L.; Agarwalla, S.; Balaram, P. *Proc. Natl. Acad. Sci. U.S.A.* **1991**, *88*, 5307.
(21) Karle, I.; Flippen-Anderson, J. L.; Agarwalla, S.; Balaram, P. *Biopolymers* **1994**, *34*, 721.
(22) Mandel-Gutfreund, Y.; Schueler, O.; Margalit, H. *J. Mol. Biol.* **1991**, *253*, 370.
(23) Binkley, J. S.; Pople, J. A.; Hehre, W. J. *J. Am. Chem. Soc.* **1980**, *102*, 939.
(24) Frey, R. F.; Coffin, J.; Newton, S. Q.; Ramek, M.; Cheng, V. K. W.; Momany, F. A.; Schäfer, L. *J. Am. Chem. Soc.* **1991**, *113*, 7129.
(25) Alemán, C.; Julia, L. *J. Phys. Chem.* **1996**, *100*, 1524.
(26) Hariharan, P. C.; Pople, J. A. *Theor. Chim. Acta* **1973**, *23*, 213.
(27) Møller, C.; Plesset, M. S. *Phys. Rev.* **1934**, *46*, 618.
(28) (a) Bachs, M.; Luque, F. J.; Orozco, M. *J. Comput. Chem.* **1994**, *15*, 446. (b) Orozco, M.; Luque, F. J. *Chem. Phys.* **1994**, *182*, 237. (c) Orozco, M.; Bachs, M; Luque, F. J. *J. Comput. Chem.* **1995**, *16*, 563s.
(29) Luque, F. J.; Bachs, M.; Orozco, M. *J. Comput. Chem.* **1994**, *15*, 847.
(30) Luque, F. J.; Negre, M. J.; Orozco, M. *J. Phys. Chem.* **1993**, *97*, 4386.
(31) Miertus, S.; Scrocco, E.; Tomasi, J. *Chem. Phys.* **1981**, *65*, 239.
(32) Miertus, S.; Tomasi, J. *Chem. Phys.* **1982**, *65*, 239.
(33) Pierotti, R. A. *Chem. Rev.* **1976**, *76*, 717.
(34) Luque, F. J.; Zhang, Y.; Alemán, C.; Bachs, M.; Gao, J.; Orozco, M. *J. Phys. Chem.* **1996**, *100*, 4269.
(35) Orozco, M.; Luque, F. J. *J. Am. Chem. Soc.* **1995**, *117*, 1378.
(36) Frisch, M. J.; Trucks, H. B.; Schlegel, H. B.; Gill, P. M. W.; Johnson, B. G.; Robb, M. A.; Cheeseman, J. R.; Keith, T.; Petersson, G. A.; Montgomery, J. A.; Raghavachari, K.; Al-Laham, M. A.; Zakrzewski, V. G.; Ortiz, V. G.; Foresman, J. B.; Peng, C. Y.; Ayala, P. Y.; Chen, W.; Wong, M. W.; Andres, J. L.; Replogle, E. S.; Gomperts, R.; Martin, R. L.; Fox, D. J.; Binkley, J. S.; Defrees, D. J.; Baker, J.; Stewart, J. J. P.; Head-Gordon, M.; Gonzalez, C.; Pople, J. A. *Gaussian 94*, Revision B.3; Gaussian, Inc.: Pittsburgh, PA, 1995.
(37) Stewart, J. J. *P. MOPAC 93*, Revision 2; Fujitsu Limited: 1993; adapted to perform MST calculations by Luque, F. J., and Orozco, M.
(38) Navas, J. J.; Alemán, C.; Muñoz-Guerra, S. *J. Org. Chem.*, in press.
(39) Alemán, C. *J. Biomol. Struct. Dyn.*, in press.
(40) Luque, F. J.; Bachs, M.; Alemán, C.; Orozco, M. *J. Comput. Chem.* **1996,** *7*, 806.
(41) Dewar, M. J. S.; Zoebisch, E. G.; Healy, E. F.; Stewart, J. J. P. *J. Am. Chem. Soc.* **1985**, *107*, 3902.
(42) Besler, B. H.; Merz, K. M.; Kollman, P. A. *J. Comput. Chem.* **1990**, *11*, 431.
(43) Gao, J.; Luque, F. J.; Orozco, M. *J. Chem. Phys.* **1993**, *98*, 2975.